Coarse-grained Monte Carlo simulations of the phase transition of the Potts model on weighted networks

Chuansheng Shen,[1,2] Hanshuang Chen,[1] Zhonghuai Hou,[1,*] and Houwen Xin[1]

[1]*Hefei National Laboratory for Physical Sciences at Microscales & Department of Chemical Physics, University of Science and Technology of China, Hefei 230026, China*
[2]*Department of Physics, Anqing Teachers College, Anqing 246011, China*

Developing an effective coarse-grained (CG) approach is a promising way for studying dynamics on large size networks. In the present work, we have proposed a strength-based CG (s-CG) method to study critical phenomena of the Potts model on weighted complex networks. By merging nodes with close strengths together, the original network is reduced to a CG network with much smaller size, on which the CG Hamiltonian can be well defined. In particular, we make an error analysis and show that our s-CG approach satisfies the condition of statistical consistency, which demands that the equilibrium probability distribution of the CG model matches that of the microscopic counterpart. Extensive numerical simulations are performed on scale-free networks and random networks, without or with strength correlation, showing that this s-CG approach works very well in reproducing the phase diagrams, fluctuations, and finite-size effects of the microscopic model, while the d-CG approach proposed in our recent work [Phys. Rev. E **82**, 011107 (2010)] does not.

I. INTRODUCTION

In the last two decades, we have witnessed dramatic advances in complex networks research, which has been one of the most active topics in statistical physics and closely related disciplines [1–3]. The central issue in this field is to study how the topology of networks influences dynamics, such as phase transition, self-organized criticality, and epidemic spreading, etc. [4–6]. Usually, Monte Carlo (MC) simulations [7] have been widely used to study such dynamics. However, the sizes of many real-world networks are very large, such as the human brain, composed of about 10^{11} neurons and 10^{14} synapses [8], and thereby brute-force simulations are quite expensive and sometimes even become impossible. Phenomenological models, such as mean-field description, may capture certain properties of the system, but often ignore microscopic details and fluctuation effects that may be important near some critical points. Therefore a promising way to bridge the gap between the microscopic details and system level behaviors is to develop coarse-grained (CG) approaches, aiming at significantly reducing the degree of freedom while properly preserving the microscopic information of interest.

Recently, several CG approaches have been proposed in the literature. Renormalization transformation has been used to reduce the size of self-similar networks while preserving the most relevant topological properties of the original ones [9–12]. Gfeller and Rios proposed a spectral decomposition technique to obtain a CG network which can reproduce the random walk and synchronization dynamics of the original network [13]. Kevrekidis *et al.* developed equation-free multiscale computational methods to accelerate simulation using a coarse time stepper [14], which has been successfully applied to study the CG dynamics of oscillator networks [15], gene regulatory networks [16], and adaptive epidemic networks

[17]. Nevertheless, none of the works mentioned above has considered critical phenomena in complex networks, which has been a frontier topic in the context of network science [6].

Very recently, we have proposed a degree-based CG (d-CG) approach to study the critical phenomena of the Ising model and the susceptible-infected-susceptible epidemic model on unweighted networks [18]. A local mean-field (LMF) scheme was introduced to generate the CG network from the microscopic one. Specifically, we have proposed a so-called condition of statistical consistency (CSC) that the CG model should satisfy to guarantee the validity of the CG approach. We showed that the CSC can be exactly fulfilled if we merge nodes with the same degree together. Extensive numerical simulations showed that our d-CG approach does work very well to reproduce the phase transition behaviors of the original network, including the critical point and the fluctuation properties, but with much less computational effort. Our method also makes it feasible to investigate the finite size effects of both models, which should be much more expensive and even forbidden if we use brute-force methods. However, this d-CG approach can only apply to binary networks, i.e., each of the link in the network either exists or not, but with no weight. As we know, many real-world networks are intrinsically weighted, with their links having diverse strengths. Examples include the collaboration networks [19–21], airport networks [22,23], metabolic networks [24], and predator-prey relationship networks [25], to list just a few. Therefore a straightforward question is can we use CG approaches to study the critical phenomena in weighted networks?

To answer this question, in the present work, we have considered the critical phenomena of the Potts model in weighted complex networks. The Potts model is related to a number of important topics in statistical and mathematical physics [26,27] and was successfully applied to neural networks, multiclass classification problems, the graph coloring problem, and so on. It contains a system of coupled nodes, each of which has p possible states. Only when two nodes

*hzhlj@ustc.edu.cn

are in the same state do they have pairwise interactions. With the increment of temperature, the Potts model undergoes an order-disorder phase transition at some critical temperature. For $p = 2$, the Potts model is equivalent to the well-known Ising model [6,26]. Instead of the d-CG scheme, we have proposed a strength-based CG (s-CG) approach, where those nodes with *similar* strengths are merged together to form a CG node. Note that in weighted networks, it is impractical to merge nodes with exactly the same strength together. By detailed analysis of the discrepancy between the Hamiltonian of a CG configuration and that of its corresponding microscopic configurations, we show that the s-CG approach can approximately satisfy the CSC defined on weighted networks. Extensive numerical simulations are performed on scale-free (SF) networks and random networks, without or with strength correlation, showing that our s-CG approach works very well in reproducing the phase diagrams, fluctuations, and finite size effects of the microscopic model, while the simple d-CG does not. Compared to our previous work [18], the present study steps forward several important steps. First of all, we should note that s-CG is a brand new method compared to d-CG and the latter cannot apply to weighted networks, although they share some similar ideas. Second, weighted networks are of more ubiquitous importance than binary unweighted ones, thus the s-CG approach should find more applications. What is more, we have extended the study from the simple two-state Ising model to a more general one, the multistate Potts model. In addition, we have performed error analysis in the present study, which clearly demonstrates the robustness of our approach.

II. COARSE-GRAINING PROCEDURE

A. CG Potts model

In this paper, we consider the p-state Potts model on a weighted network consisting of N nodes, whose Hamiltonian is given by

$$H = -\sum_{i<j} w_{ij}\delta_{\alpha_i,\alpha_j}, \tag{1}$$

where w_{ij} is the weight on the edge connecting a pair of nodes i and j ($w_{ij} = 0$ if the nodes i and j are not connected). $\alpha_i \in \{1,\ldots,p\}$ denotes the state of node i, and $\delta_{\alpha_i,\alpha_j} = 1$ if $\alpha_i = \alpha_j$ and 0 otherwise.

To set up the CG Potts model, one needs to obtain the CG Hamiltonian defined on the CG network, followed by CG MC simulations to study the dynamic behaviors. The CG network is simply obtained by node merging, i.e., q_μ nodes within the original micronetwork are merged into a single CG node C_μ, where $\mu = 1,\ldots,N^c$ labels the CG node and N^c is the size of the CG network. Following the LMF scheme used in [18], the weight of the edge between two CG nodes μ and ν reads

$$\bar{w}_{\mu\nu} = \begin{cases} \dfrac{2}{q_\mu(q_\mu - 1)} \displaystyle\sum_{i,j \in C_\mu; i<j} w_{ij} & \text{for } \mu = \nu, \\[4mm] \dfrac{1}{q_\mu q_\nu} \displaystyle\sum_{i \in C_\mu, j \in C_\nu} w_{ij} & \text{for } \mu \neq \nu. \end{cases} \tag{2}$$

The CG Hamiltonian $\bar{H}$ can be readily obtained,

$$\bar{H} = \bar{H}_1 + \bar{H}_2,$$

where

$$\bar{H}_1 = -\sum_\mu \bar{w}_{\mu\mu} \sum_\alpha \frac{\eta_{\mu,\alpha}(\eta_{\mu,\alpha} - 1)}{2}, \tag{3a}$$

$$\bar{H}_2 = -\sum_{\mu,\nu(>\mu)} \bar{w}_{\mu\nu} \sum_\alpha \eta_{\mu,\alpha}\eta_{\nu,\alpha}. \tag{3b}$$

Herein, $\bar{H}_1$ ($\bar{H}_2$) denotes CG interactions inside (among) the CG nodes, respectively. $\eta_{\mu,\alpha}$ stands for the number of α-state micronodes inside C_μ. Since there are $\frac{\eta_{\mu,\alpha}(\eta_{\mu,\alpha}-1)}{2}$ possible distinct pairs of α-state micronodes inside C_μ, and each pair has a weighted coupling $\bar{w}_{\mu\mu}$, the CG interactions among all the α-state nodes inside C_μ are given by

$$\bar{H}_{\mu,1}^{(\alpha)} = -\bar{w}_{\mu\mu} \frac{\eta_{\mu,\alpha}(\eta_{\mu,\alpha} - 1)}{2}.$$

Summation of this over all CG nodes μ and states α gives the result in Eq. (3a). Equation (3b) can be interpreted in a similar way. Note that Eqs. (3) are closed at the CG level, i.e., as long as one has constructed the CG network, $\bar{w}$ and $\bar{H}$ are then both well defined, based on which one can perform CG-MC simulations without going back to the microlevel.

B. CSC

The above procedure indicates how to calculate the CG Hamiltonian if we already have the CG network. However, which q_μ nodes are merged together to form a CG node C_μ is yet not determined. Generally speaking, one may construct the CG network deliberately, for instance, one may simply generate N^c values, q_μ, obeying $\sum_{\mu=1}^{N^c} q_\mu = N$ and then just randomly merge q_μ micronodes to form C_μ. Therefore an important question arises: How do we guarantee that the CG model can reproduce the dynamics of the corresponding microscopic model correctly?

We address this problem by extending the so-called CSC as proposed in [18]. We introduce $\vec{\eta}_\mu = \{\eta_{\mu,\alpha}\}_{\alpha=1,\ldots,p}$ to denote the state of C_μ and $\vec{\eta} = \{\vec{\eta}_\mu\}_{\mu=1,\ldots,N^c}$ to denote the configuration of the CG network. Note that a given CG configuration $\vec{\eta}$ corresponds to many microscopic configurations, which defines the degeneracy factor $g(\vec{\eta})$. In the equilibrium state of the CG model, the probability of finding a given CG configuration $\vec{\eta}$ is given by the canonical distribution, i.e.,

$$p_{\text{CG}}(\vec{\eta}) = g(\vec{\eta})e^{-\bar{H}/k_BT}/\bar{Z},$$

where $\bar{Z} = \sum_{\vec{\eta}} p_{\text{CG}}(\vec{\eta})$ is the CG partition function, k_B is the Boltzmann constant, and T is temperature. It is important to note, however, that $p_{\text{CG}}(\vec{\eta})$ can be calculated exactly from the equilibrium distribution of the micromodel,

$$p_{\text{micro}}(\vec{\eta}) = \sum{}' e^{-H/k_BT}/Z,$$

where Z is the partition function of the micromodel, and the prime means summation over all the microscopic configurations that contribute to $\vec{\eta}$. Since we are interested in the equilibrium phase transition behavior of the Potts model, we thus assert that for the CG model to be statistically consistent

with the micromodel, $p_{CG}(\vec{\eta})$ and $p_{micro}(\vec{\eta})$ must be equal, i.e., the CSC reads

$$g(\vec{\eta})e^{-\bar{H}/k_B T}/\bar{Z} = \sum{}' e^{-H/k_B T}/Z. \qquad (4)$$

C. s-CG scheme and error analysis

In the present work, we propose a s-CG scheme to construct the CG network, i.e., nodes with the same or similar strengths are merged together to form a CG node, where the strength s_i of node i is defined as $s_i = \sum_j w_{ij}$ [22,28]. In the following, we will show that if nodes inside each CG node have the same strength, the CSC will hold exactly within the annealed network approximation (ANA) [6,29–31]. In addition, if the strengths within C_μ are nearly the same, the CSC can also hold approximately.

ANA has been widely used to study the ensemble averaged dynamics of complex networks and proved to be successful. ANA assumes that one can replace the dynamics on a given network by that on a weighted fully connected graph with connectivity $A_{ij} = d_i d_j/(DN)$, where d_i (d_j) denotes the degree of node i (j) and D is the mean degree of the network. Analogously, in weighted networks link weight can be expressed as

$$w_{ij} = s_i s_j/(SN), \qquad (5)$$

where S is the mean strength of the network. Substituting Eq. (5) into Eq. (2), the adjacency matrix of the CG network now reads

$$\bar{w}_{\mu\mu} = \frac{2}{q_\mu(q_\mu - 1)} \sum_{i<j \in C_\mu} \frac{(S_\mu + \delta s_i)(S_\mu + \delta s_j)}{SN}$$

$$= \frac{S_\mu^2}{SN}(1 - \Omega_\mu), \qquad (6a)$$

$$\bar{w}_{\mu\nu} = \frac{1}{q_\mu q_\nu} \sum_{i \in C_\mu, j \in C_\nu} \frac{(S_\mu + \delta s_i)(S_\nu + \delta s_j)}{SN} = \frac{S_\mu S_\nu}{SN}. \qquad (6b)$$

Herein, we have written $s_i = S_\mu + \delta s_i$, with $S_\mu = \frac{1}{q_\mu} \sum_{i \in C_\mu} s_i$ being the mean strength within C_μ. $\Omega_\mu = \frac{\langle \delta s^2 \rangle_\mu}{S_\mu^2(q_\mu - 1)}$ where $\langle \delta s^2 \rangle_\mu = \frac{1}{q_\mu} \sum_{i \in C_\mu} (\delta s_i)^2$ is the variance of strengths within C_μ. In Eq. (6a), we have used the fact that $(\sum_{i \in C_\mu} \delta s_i)^2 = 2 \sum_{i<j \in C_\mu} \delta s_i \delta s_j + \sum_{i \in C_\mu} (\delta s_i)^2 = 0$. Equation (6b) holds simply because $\sum_{i \in C_\mu, j \in C_\nu} \delta s_i \delta s_j = (\sum_{i \in C_\mu} \delta s_i)(\sum_{j \in C_\nu} \delta s_j) = 0$. Substituting Eq. (6) into Eq. (3), we can get

$$\bar{H}_1 = -\frac{1}{SN} \sum_\mu S_\mu^2 (1 - \Omega_\mu) \sum_\alpha \frac{\eta_{\mu,\alpha}(\eta_{\mu,\alpha} - 1)}{2}, \qquad (7a)$$

$$\bar{H}_2 = -\frac{1}{SN} \sum_{\mu,\nu(>\mu)} S_\mu S_\nu \sum_\alpha \eta_{\mu,\alpha} \eta_{\nu,\alpha}. \qquad (7b)$$

To compare the CG Hamiltonian with the microscopic one, we now group the micronodes with same state α inside C_μ as $C_{\mu,\alpha}$. Clearly, the size of $C_{\mu,\alpha}$ is $\eta_{\mu,\alpha}$. As in Eq. (3), we can also split the micro-Hamiltonian H into two parts,

$$H = H_1 + H_2, \qquad (8)$$

where H_1 and H_2 denote energy contributions from intra- and inter-CG nodes, respectively. With ANA, and noting the fact only nodes with same state have interactions at the microlevel, one has

$$H_1 = -\sum_\mu \sum_\alpha \sum_{i<j \in C_{\mu,\alpha}} \frac{s_i s_j}{SN} \frac{\eta_{\mu,\alpha}(\eta_{\mu,\alpha} - 1)}{2}, \qquad (9a)$$

$$H_2 = -\sum_{\mu,\nu(>\mu)} \sum_\alpha \sum_{i \in C_{\mu,\alpha}, j \in C_{\nu,\alpha}} \frac{s_i s_j}{SN} \eta_{\mu,\alpha} \eta_{\nu,\alpha}. \qquad (9b)$$

Following similar steps to obtain Eq. (7), we may also write $s_i = S_{\mu,\alpha} + \delta s_i$ (here node i belongs to the group $C_{\mu,\alpha}$) and Eqs. (9) change to

$$H_1 = -\sum_\mu \sum_\alpha \sum_{i<j \in C_{\mu,\alpha}} \frac{(S_{\mu,\alpha} + \delta s_i)(S_{\mu,\alpha} + \delta s_j)}{SN}$$

$$\times \frac{\eta_{\mu,\alpha}(\eta_{\mu,\alpha} - 1)}{2}$$

$$= -\frac{1}{SN} \sum_\mu \sum_\alpha S_{\mu,\alpha}^2 (1 - \Omega_{\mu,\alpha}) \frac{\eta_{\mu,\alpha}(\eta_{\mu,\alpha} - 1)}{2}, \quad (10a)$$

$$H_2 = -\sum_{\mu,\nu(>\mu)} \sum_\alpha \sum_{i \in C_{\mu,\alpha}, j \in C_{\nu,\alpha}} \frac{(S_{\mu,\alpha} + \delta s_i)(S_{\nu,\alpha} + \delta s_j)}{SN} \eta_{\mu,\alpha} \eta_{\nu,\alpha}$$

$$= -\frac{1}{SN} \sum_{\mu,\nu(>\mu)} \sum_\alpha \eta_{\mu,\alpha} \eta_{\nu,\alpha} S_{\mu,\alpha} S_{\nu,\alpha}. \qquad (10b)$$

Here $\Omega_{\mu,\alpha} = \frac{\langle \delta s^2 \rangle_{\mu,\alpha}}{S_{\mu,\alpha}^2(\eta_{\mu,\alpha} - 1)}$ where $\langle \delta s^2 \rangle_{\mu,\alpha} = \frac{1}{\eta_{\mu,\alpha}} \sum_{i \in C_{\mu,\alpha}} (\delta s_i)^2$ is the variance of strengths within the group of nodes $C_{\mu,\alpha}$. Comparing Eqs. (7) with Eqs. (10), the discrepancy between the CG Hamiltonian and the micro-Hamiltonian is given by

$$\bar{H}_1 - H_1 = -\frac{1}{SN} \sum_\mu \sum_\alpha \frac{\eta_{\mu,\alpha}(\eta_{\mu,\alpha} - 1)}{2}$$

$$\times \left[S_\mu^2 (1 - \Omega_\mu) - S_{\mu,\alpha}^2 (1 - \Omega_{\mu,\alpha}) \right], \quad (11a)$$

$$\bar{H}_2 - H_2 = -\frac{1}{SN} \sum_{\mu,\nu} \sum_\alpha \eta_{\mu,\alpha} \eta_{\nu,\alpha} (S_\mu S_\nu - S_{\mu,\alpha} S_{\nu,\alpha}). \quad (11b)$$

Obviously, for the exact s-CG algorithm where all the nodes inside a given CG node have same strength, $\Omega_\mu = \Omega_{\mu,\alpha} = 0 \, \forall (\mu,\alpha)$ and $S_\mu = S_{\mu,\alpha}$, hence $\bar{H}_1 = H_1$ and $\bar{H}_2 = H_2$. In this case, all those microscopic configurations contributing to a CG configuration $\vec{\eta}$ have exactly the same Hamiltonian H, which also is equal to the CG Hamiltonian $\bar{H}$. Since the constrained summation $\sum{}'$ contains exactly $g(\vec{\eta})$ items, the numerators on both sides of Eq. (4) are exactly equal, i.e., $g(\vec{\eta})e^{-\bar{H}/k_B T} = \sum{}' e^{-H/k_B T}$. Since we can also write the microscopic partition function as $Z = \sum_{\vec{\eta}}(\sum{}' e^{-H/k_B T})$, it is readily shown that the two partition functions are equal, $\bar{Z} = Z$. Therefore the CSC, Eq. (4), exactly holds.

However, we should note that for a weighted network, the exact s-CG method is not practical, since the strength of a given node is generally not an integer. Therefore usually one can only merge nodes with close strengths together. Let us analyze Eq. (11) again. The factor Ω_μ scales as $\frac{\langle \delta s^2 \rangle_\mu}{S_\mu^2 q_\mu}$, hence if
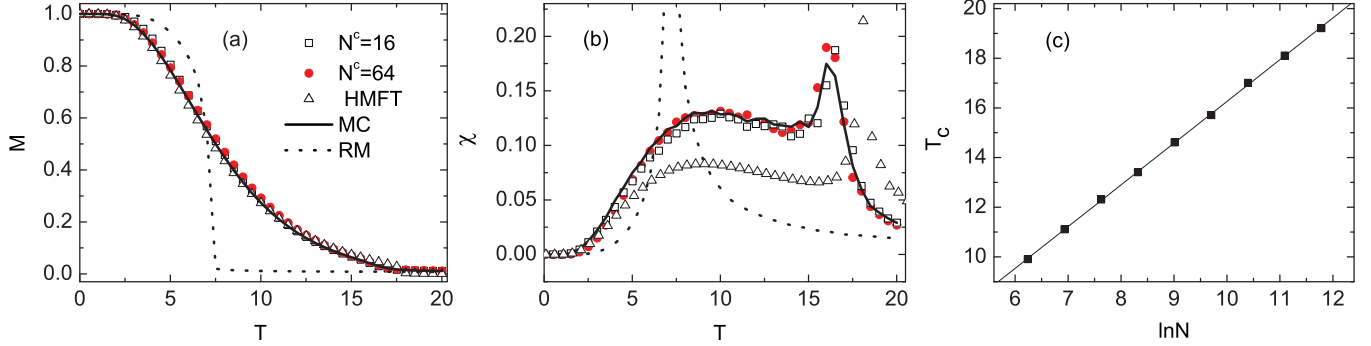
FIG. 1. (Color online) (a), (b) M and χ as functions of T for the three-state Potts model on unweighted SF networks ($N = 16384$ and $\theta = 0$), obtained from MC simulation (solid line), HMFT (triangle), random-merging CG (dotted line), and the s-CG (square and circle). (c) Dependence of T_c on the network size N obtained from the s-CG approach with the fixed $N^c = 64$. All the networks have the fixed $D = 20$. The error bars (not shown) are smaller than the symbol sizes.

we merge many nodes with similar strengths together, $\Omega_\mu \ll 1$ is expected to be true. One may also expect that $\Omega_{\mu,\alpha} \ll 1$ for the same reason. Therefore the discrepancy between $\bar{H}$ and H mainly depends on the difference between S_μ and $S_{\mu,\alpha}$. Here, we note that the nodes with α state flip with time during the simulation. In the equilibrium state, one expects that $C_{\mu,\alpha}$ may scan throughout C_μ many times, such that $S_{\mu,\alpha}$ averaged over time is close to S_μ. Hence $(\bar{H} - H)/H$ averaged over long time could be small. Note that if we merge nodes randomly, $\Omega_\mu \ll 1$ and $\Omega_{\mu,\alpha} \ll 1$ will be violated and the above reasoning should fail. We thus conclude that the pratical s-CG approach, by merging nodes with similar strengths together, can satisfy the CSC approximately.

III. NUMERICAL RESULTS

To show the validity of our s-CG approach, we perform extensive simulations on weighted SF networks. SF networks are very heterogeneous and serve as better candidates to test our method than other homogeneous networks, such as small-world or random networks (other types of complex networks have also been investigated; the qualitative results are the same and not shown here). We first generate a standard (unweighted) SF network by using the Barabási-Albert (BA) model [32] with power-law degree distribution $P(k) \sim k^{-3}$. To convert this unweighted SF network into a weighted one, we use the algorithm as proposed in [33]: The weight of a link between node i and j ($1 \leqslant i, j \leqslant N$) is given by $w_{ij} = (\frac{i}{N} + \frac{j}{N})^\theta/2$, where the indexes of all nodes have been randomly shuffled and θ is a tunable parameter. Note that $\theta = 0$ corresponds to an unweighed network.

The MC simulation at the microscopic level follows standard Metropolis dynamics: At each step, we randomly selected a micronode and try to update its state to another state randomly chosen from the other possible $p - 1$ states, with an acceptance probability $\min(1, e^{-\Delta H/k_B T})$, where ΔH is the associated change of the micro-Hamiltonian. In the present work, we set $k_B = 1$. Similarly, during each CG-MC step, a CG node C_μ is randomly chosen with a probability proportional to its size q_μ. The probability for the process that an α node changes to a β node, with correspondingly $\eta_{\mu,\alpha} \to \eta_{\mu,\alpha} - 1$ and $\eta_{\mu,\beta} \to \eta_{\mu,\beta} + 1$, is given by $\eta_{\mu,\alpha} \min(1, e^{-\Delta \bar{H}/k_B T})$, where

$\Delta \bar{H}$ is the change of CG Hamiltonian during this process. Since N^c can be much smaller than N, the CG MC is expected to be much faster and memory saving than the microlevel MC simulation.

The collective state of the system is described by the total magnetic moment $M = \frac{1}{2N} \sum_{\mu,\alpha} |M_{\mu,\alpha}|$, where $M_{\mu,\alpha} = \frac{p\eta_{\mu,\alpha}-1}{p-1}$ ($\mu = 1, \ldots, N^c$) denotes the α component of the magnetic moment within C_μ. With increasing temperature T, the Potts model undergoes a phase transition at some critical temperature T_c from an ordered state, where $M \sim O(1)$ is strictly nonzero, to a disordered state with $M \simeq 0$. We use the similar s-CG approach to construct the CG network with different N^c and compare the results obtained from CG-MC simulations with those of micro-MC simulations.

To begin, we consider the three-state Potts model. In Fig. 1, we show the results for $\theta = 0$, where the network is essentially unweighted and the s-CG approach is identical to the d-CG. Figures 1(a) and 1(b) show the moment M and susceptibility $\chi = \beta N(\langle M^2 \rangle - \langle M \rangle^2)$ as functions of T, respectively. The susceptibility is related to the variance of the total magnetization according to the fluctuation-dissipation theorem. Apparently, our CG results (empty squares and solid circles) are in excellent agreement with the microlevel counterparts (solid lines). As comparisons, we have also shown the results obtained by a random-merging (RM) CG model (dotted lines) and the heterogeneous mean-field theories (HMFT) [34] (empty triangles). Here, the RM model means that one simply merges N/N^c randomly selected nodes to form a CG node. Evidently this random scheme fails to reproduce the microscopic behaviors at all. The results of the HMFT are obtained by numerically solving the self-consistent equations of order parameter [34]. We find that the HMFT can predict the curve of $M \sim T$ quite well, however, it fails to predict the curve of $\chi \sim T$. Strikingly, even when the original network is reduced to one with only 16 CG nodes, the CG model still faithfully reproduces the phase transition curves and fluctuation properties. Since N^c is largely reduced compared to N, a considerable speedup of CPU time can be achieved, which makes it feasible to study system size effects. Figure 1(c) plots T_c as a function of $\ln N$, obtained by our CG method with $N^c = 64$. T_c is determined as the location of the peak in the $\chi \sim T$ curve, as in Fig. (1(b)). The dependence
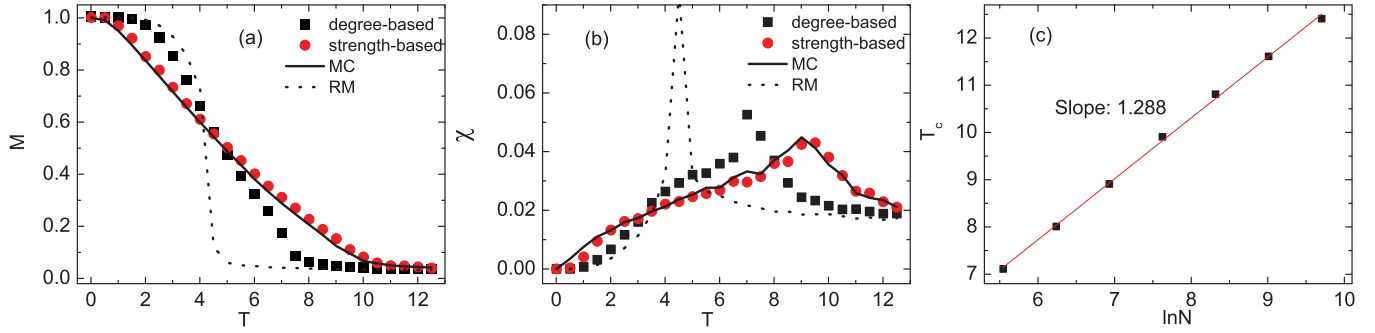
FIG. 2. (Color online) (a), (b) M and χ as functions of T for the three-state Potts model on weighted SF networks with $D = 20$, $N = 1024$, $\theta = 2.4$, and $N^c = 16$. (c) Dependence of T_c on the network size N. The error bars are omitted for clarify since they are smaller than the symbol sizes.

is linear with a slope $\simeq 1.68$, which agrees rather well with a theoretical prediction $T_c / \ln N = \frac{S}{4p} \simeq 1.67$ [34], where S is the average node strength in the network.

For $\theta \neq 0$, the networks are weighted. Here we take $\theta = 2.4$ as an example to ensure the heterogeneity of the link weights. Figures 2(a) and 2(b) show M and χ as functions of T, respectively. As in Fig. 1(b), the peak in χ locates the critical point T_c. Clearly, the s-CG results (solid circle) are still in excellent agreement with the MC results (solid lines), however, the d-CG (solid squares) [18] and RM CG (dotted lines) both fail. For such weighted networks, the dynamic equations of HMFT is not available either. Thus, for such weighted networks, our s-CG approach is the only promising CG approach so far. In Fig. 2(c), we have also shown the dependence of T_c on the network size N. Apparently, there is also a linear dependence between T_c and $\ln N$ with the slope being about 1.288. As mentioned in the former paragraph, this slope depends on the average strength S. For a weighted network, one may estimate S by $\langle w_{ij} \rangle D$, where $\langle w_{ij} \rangle \simeq \int_0^2 x^\theta / 4 dx = \frac{1}{4(\theta+1)} 2^{\theta+1}$. Substituting $D = 20$, $\theta = 2.4$, and $p = 3$ to these formula, we obtain $T_c / \ln N = \frac{S}{4p} \simeq 1.293$, which is consistent with the simulation value.

In real-world networks, correlation is an ubiquitous feature. For instance, social networks show that nodes with large degrees tend to connect together, a property referred to as "assortative mixing" [35]. In contrast, many technological and biological networks show "disassortative mixing," i.e., connections between high-degree and low-degree nodes are more probable [36,37]. Previous studies showed that correlations may play important roles in network dynamics [35–39]. In the present work, we have used our s-CG method to study the phase transition of the Potts model on correlated networks, which cannot be studied by the HMFT, which assumes no degree correlation. To characterize the assortative property of the weighted network, a strength correlation coefficient r, an extension of the degree correlation [35], can be defined as

$$r = (\langle s_i s_j \rangle - \langle s_i \rangle \langle s_j \rangle) / (\langle s_i^2 \rangle - \langle s_i \rangle^2). \quad (12)$$

Here s_i and s_j are the strengths of the two end nodes of an edge. r is zero for networks with no strength correlation, such as BA-SF networks, and positive or negative for assortative or disassortative mixing networks, respectively.

Figure 3(a) shows T_c as a function of r, obtained from our s-CG approach and micro-MC simulations for $\theta = 0$. Again, the fits between CG-MC and MC are good. Figure 3(b) shows the effects of correlated network size on T_c. Interestingly, we find that the linear dependence between T_c and $\ln N$ is lost for correlated networks. For assortative (disassortative) networks T_c grows monotonically much faster (slower) than $\ln N$, respectively. In other words, the ordered state in an assortative (disassortative) network is harder (easier) to be destroyed with increasing temperature than in an uncorrelated network. This is understandable since a "hub" node in the network is more difficult to change its state than a "leaf node due to a larger energy barrier. In an assortative network, hub nodes are connected together, such that they tend to freeze into a local ordered state which is stable to thermal fluctuations. For a disassortative network, a hub node is usually connected to many leaf nodes. Since leaf nodes can change state easily, the "alone" hub node is more likely to change state with the help of their "boiling" neighbors. Therefore assortative correlations tend to increase T_c as observed here.

In Fig. 4, M and χ of the three-state Potts model on weighted networks are plotted as functions of T at different correlation coefficient r, obtained from our s-CG approach and micro-MC simulations. Again, the agreements between CG-MC and MC are excellent, further demonstrating the validity of our method.
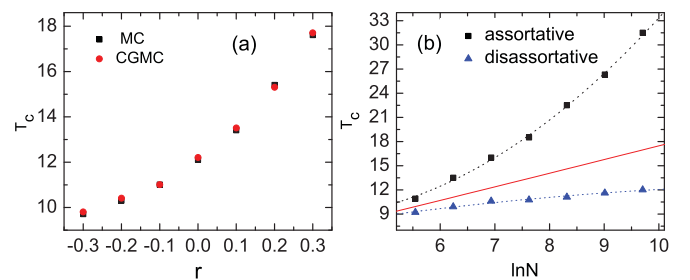

FIG. 3. (Color online) Phase transition behaviors of the three-state Potts model on unweighted correlated networks. (a) T_c plotted as a function of the network correlation coefficient r, obtained via CG-MC and MC simulations, with $N = 1024$ and $N^c = 64$. (b) Dependence of T_c on the network size N. The solid line corresponds to uncorrelated networks for comparison. All the networks have the fixed $D = 20$.
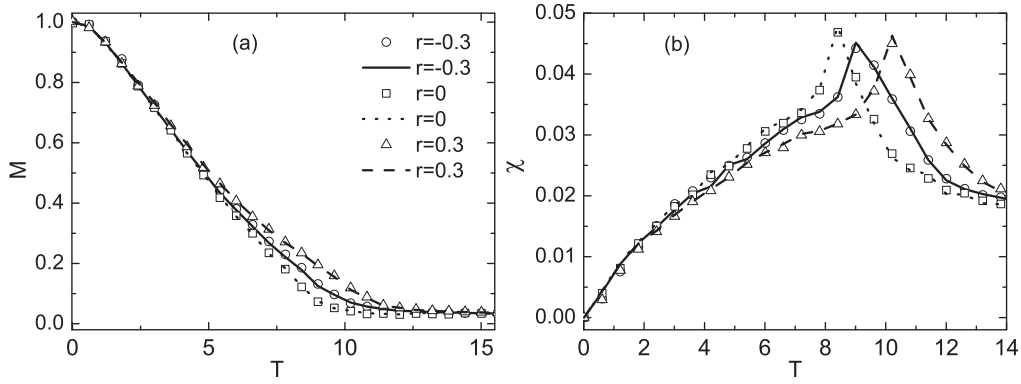
FIG. 4. M and χ as functions of T for the three-state Potts model on weighted correlated networks. The symbols and lines correspond to the CG-MC and MC simulation results, respectively. Other parameters are the same as in Fig. 2.

So far, we have shown that our CG model can faithfully reproduce the phase transition of the $p = 3$ states Potts model. In the following, we will demonstrate the validity of our CG approach for the general p-state Potts model. It was known that the order of the phase transition for the p-state Potts model in regular lattices depends on both p and dimensionality. In two-dimensional lattices, the transition is first order for $p \geqslant 5$,

while in three-dimensional lattices the transition is first order for $p \geqslant 3$ [26]. For the networked p-state Potts model, it was shown that the first-order phase transition is suppressed as the degree distribution of a network becomes more heterogeneous [34,40,41]. In Fig. 5(a) and 5(b), we plot M and χ as functions of T for the p-state Potts model with $p = 5, 8, 12$ on weighted BA networks. It is clearly observed that there are good
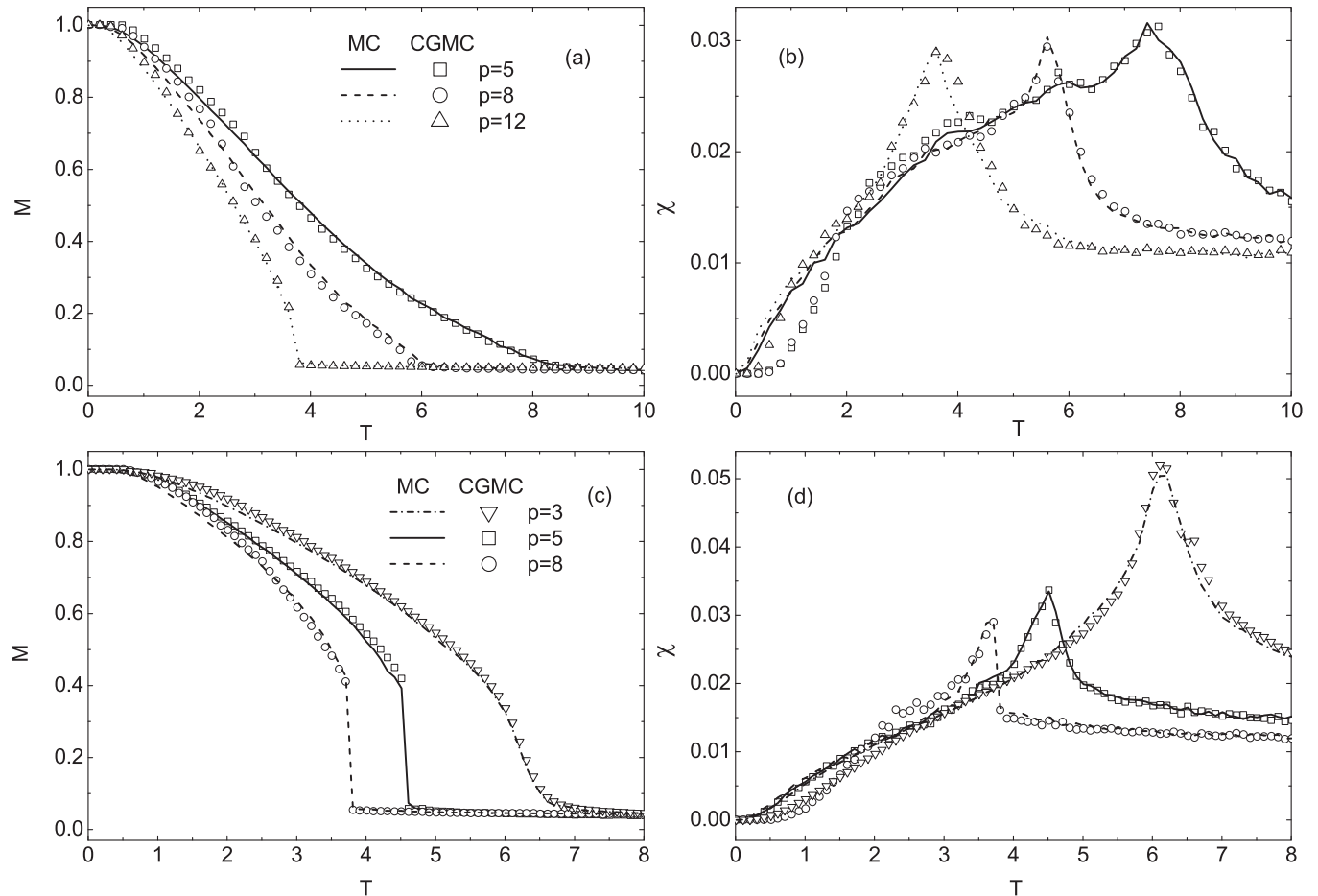

FIG. 5. M and χ as functions of T for the p-state Potts model: (a), (b) correspond to weighted BA networks, and (c), (d) to weighted ER networks. The symbols and lines in (b) are the same as (a), and the symbols and lines in (d) are the same as (c). Other parameters are the same as in Fig. 2.

agreements between CG-MC simulations and MC simulations. It is also found that the jump of magnetization at the phase transition, a signature of a first-order transition, is not profound even for $p = 12$. However, it is expected that the first-order phase transition will appear in a more homogeneous network. To the end, we consider a well-known homogeneous network model, Erdös-Rényi (ER) random networks, to test the feasibility of our CG approach in the first-order phase transition. In Figs. 5(c) and 5(d), we plot M and χ as functions of T for the p-state Potts model with $p = 3, 5, 8$ on weighted ER networks. The agreements between CG-MC and MC are good, and the results show that for $p = 3$ the phase transition is second order, while for $p = 5$ and $p = 8$ the phase transition is first order.

IV. CONCLUSIONS

In summary, we have developed a s-CG approach for studying the phase transition of the Potts model on weighted networks. We have utilized a LMF scheme to generate the connectivity of the CG network and derived the CG Hamiltonian. To address the problem of how to guarantee the validity of the CG model, we have proposed the so-called CSC, which requires that the probability to find a given CG configuration in the equilibrium state, calculated from the CG model, should be the same as that calculated from the original microscopic model. We show, by performing error analysis, that our s-CG approach, by merging nodes with close strengths together, holds the CSC approximately with ANA. Detailed numerical simulations demonstrate clearly that our s-CG approach can reproduce the microscopic MC simulation results very well, not only for the onset of phase transition, but also for the fluctuations and system size effects.

[1] R. Albert and A.-L. Barabási, Rev. Mod. Phys. **74**, 47 (2002).

[2] S. N. Dorogovtsev and J. F. F. Mendes, Adv. Phys. **51**, 1079 (2002).

[3] M. Newman, SIAM Rev. **45**, 167 (2003).

[4] S. Boccaletti, V. Latora, Y. Moreno, M. Chavez, and D.-U. Hwang, Phys. Rep. **424**, 175 (2006).

[5] A. Arenas, A. Díaz-Guilera, J. Kurths, Y. Moreno, and C. Zhou, Phys. Rep. **469**, 93 (2008).

[6] S. N. Dorogovtsev, A. V. Goltsev, and J. F. F. Mendes, Rev. Mod. Phys. **80**, 1275 (2008).

[7] D. P. Landau and K. Binder (Cambridge University Press, Cambridge, England, 2000).

[8] M. I. Rabinovich, P. Varona, A. I. Selverston, and H. D. I. Abarbanel, Rev. Mod. Phys. **78**, 1213 (2006).

[9] B. J. Kim, Phys. Rev. Lett. **93**, 168701 (2004).

[10] C. Song, S. Havlin, and H. A. Makse, Nature (London) **433**, 392 (2005).

[11] K. I. Goh, G. Salvi, B. Kahng, and D. Kim, Phys. Rev. Lett. **96**, 018701 (2006).

[12] F. Radicchi, J. J. Ramasco, A. Barrat, and S. Fortunato, Phys. Rev. Lett. **101**, 148701 (2008).

[13] D. Gfeller and P. De Los Rios, Phys. Rev. Lett. **100**, 174104 (2008).

[14] I. G. Kevrekidis, C. W. Gear, J. M. Hyman, P. G. Kevrekidis, O. Runborg, and C. Theodoropoulos, Commun. Math. Sci. **1**, 715 (2003).

[15] S. J. Moon, R. Ghanem, and I. G. Kevrekidis, Phys. Rev. Lett. **96**, 144101 (2006).

[16] R. Erbana, I. G. Kevrekidis, D. Adalsteinsson, and T. C. Elston, J. Chem. Phys. **124**, 084106 (2006).

[17] T. Gross and I. G. Kevrekidis, Eur. Phys. Lett. **82**, 38004 (2008).

[18] H. S. Chen, Z. H. Hou, H. W. Xin, and Y. J. Yan, Phys. Rev. E **82**, 011107 (2010).

[19] M. E. J. Newman, Phys. Rev. E **64**, 016131 (2001).

[20] M. E. J. Newman, Phys. Rev. E **64**, 016132 (2001).

[21] A.-L. Barabási, H. Jeong, Z. Néda, E. Ravasz, A. Schubert, and T. Vicsek, Physica A **311**, 590 (2002).

[22] A. Barrat, M. Barthlemy, R. Pastor-Satorras, and A. Vespignani, Proc. Natl. Acad. Sci. U.S.A. **101**, 3747 (2004).

[23] E. Almaas, P. L. Krapivsky, and S. Redner, Phys. Rev. E **71**, 036124 (2005).

[24] E. Almaas, B. Kovcs, T. Viscek, Z. N. Oltval, and A. L. Barabsi, Nature (London) **427**, 839 (2004).

[25] S. L. Pimm, *Food Webs*, 2nd ed. (The University of Chicago Press, Chicago, 2002).

[26] F. Y. Wu, Rev. Mod. Phys. **54**, 235 (1982).

[27] M. A. Garey and D. S. Johnson, *Computers and Intractability* (Freeman, New York, 1979).

[28] S. H. Yook, H. Jeong, A.-L. Barabsi, and Y. Tu, Phys. Rev. Lett. **86**, 5835 (2001).

[29] M. Boguñá and R. Pastor-Satorras, Phys. Rev. E **68**, 036112 (2003).

[30] G. Caldarelli, A. Capocci, P. De Los Rios, and M. A. Munoz, Phys. Rev. Lett. **89**, 258702 (2002).

[31] R. Pastor-Satorras and A. Vespignani, Phys. Rev. E **65**, 035108R (2002).

[32] A.-L. Barabási and R. Albert, Science **286**, 509 (1999).

[33] K. Park, Y. C. Lai, and N. Ye, Phys. Rev. E **70**, 026109 (2004).

[34] S. Dorogovtsev, A. Goltsev, and J. Mendes, Eur. Phys. J. B **38**, 177 (2004).

[35] M. E. J. Newman, Phys. Rev. Lett. **89**, 208701 (2002).

[36] R. Pastor-Satorras, A. Vázquez, and A. Vespignani, Phys. Rev. Lett. **87**, 258701 (2001).

[37] S. Maslov and K. Sneppen, Science **296**, 910 (2002).

[38] A. V. Goltsev, S. N. Dorogovtsev, and J. F. F. Mendes, Phys. Rev. E **78**, 051105 (2008).

[39] M. Boguna and R. Pastor Satorras, Phys. Rev. E **66**, 047104 (2002).

[40] F. Iglói and L. Turban, Phys. Rev. E **66**, 036140 (2002).

[41] M. Karsai, J.-C. Angles d'Auriac, and F. Iglói, Phys. Rev. E **76**, 041107 (2007).